Quantum Electronics **44** (10) 895–898 (2014)

LASERS

PACS numbers: 42.55.Rz; 42.70.Hj; 42.60.Lh
DOI: 10.1070/QE2014v044n10ABEH015425

Lasing in a Tm:$Yb_3Al_5O_{12}$ crystal pumped at 1.678 μm

Yu.D. Zavartsev, A.I. Zagumennyi, Yu.L. Kalachev,
S.A. Kutovoi, V.A. Mikhailov, I.A. Shcherbakov

Abstract. **The $Yb_3Al_5O_{12}$ (YbAG) crystal is proposed as a matrix of Tm^{3+}-doped laser elements for two-micron lasers. A Tm:YbAG crystal of high optical quality is grown by the Czochralski method and its spectral and luminescent characteristics are studied. The luminescence decay time for the upper laser level $^3F_4$ is measured to be 4.7 ms. Lasing in this crystal pumped by a 1.678-μm fibre laser is obtained at a wavelength of 2.02 μm for the first time. The total and slope efficiencies of the laser at room temperature and an output power up to 330 mW reach 33% and 41%, respectively.**

Keywords: *Tm, YbAG, laser, luminescence, lasing, lifetime.*

1. Introduction

Two-micron lasers based on different crystals doped with Tm^{3+} ions find multiple applications in different fields of science and engineering [1]. However, despite a large number of crystal matrices of active elements (AEs) studied to date, search for crystals with new combinations of laser properties continues in order to extend the range of application of these lasers. For example, recently we have grown a laser-quality Tm:Sc_2SiO_5 crystal, which demonstrated a highly efficient lasing with a broad emission line near 1.98 μm [2].

The $Yb_3Al_5O_{12}$ (YbAG) crystal, which is an analogue of the $Y_3Al_5O_{12}$ (YAG) crystal with replacement of the Y atom by Yb, attracts the attention of researchers as an alternative matrix for AEs [3], in particular, for lasing in the two-micron spectral region. For the first time, interest in the Tm:YbAG crystal as a promising crystal was expressed due to efficient up-conversion processes and the possibility of lasing in the visible region [4]. The luminescence spectra of this crystal in the ranges 340–370 nm and 450–510 nm and the energy transfer upconversion were studied upon pumping by a 1-W Ti:sapphire laser at wavelengths of 925–980 nm.

In contrast to the YAG crystal, in the YbAG matrix an additional energy level exists at $E \approx 10000$ cm^{-1}, which can create a channel of excitation energy decay. We believe that this channel must not decrease the laser efficiency because, upon excitation of the $^3F_4$ level of the thulium ion, the $^5F_{5/2}$ level of ytterbium ions can be populated only via upconversion transitions, which are typical for thulium ions in any matrix. Then, the population of the $^3F_4$ level will be partially restored due to the transition from the $^5F_{5/2}$ level.

This work presents, as far as we know, for the first time the results of experiments on the growth of Tm:YbAG crystals of high optical quality, investigations of its spectral characteristics, and implementation of lasing. Laser pumping was performed into the $^3F_4$–$^3H_6$ transition.

2. Laser crystal

The growth technology of YbAG crystals is similar to the growth technology of YAG crystals. The Tm:YbAG crystals were grown by the Czochralski method from an iridium crucible with an outer diameter of 40 mm and a height of 40 mm. To prevent interaction of the melt with the crucible material, the growth occurred in the nitrogen atmosphere with addition of oxygen (99.5% N_2 + 0.5% O_2). A crystal 75 mm long and 18 mm in cross section was grown on a single crystal seed with the ⟨100⟩ orientation; the growth rate was 5.4 mm h^{-1}. The grown crystal was annealed in air at 1200 °C in order to destroy colour centres appeared during growth.

A cubic laser AE with a thulium concentration of 5.7 at. % and dimensions 3 × 3 × 3 mm was cut along the ⟨100⟩ crystallographic direction. The opposite faces of the crystal were parallel with an accuracy no worse than 10″. The crystal faces were not antireflection coated. The AE was mounted so that it had a good thermal contact with a copper heat sink plate. The experiments were performed at room temperature.

3. Spectral characteristics

The diagram of low-lying levels of Tm^{3+} and Yb^{3+} ions is presented in Fig. 1. Since we failed to find data on the energy level diagram of Tm^{3+} in the YbAG matrix, we present the diagram of Tm^{3+} levels in YAG taken from [5] and the energy level diagram of Yb^{3+} from [6]. The absorption spectrum of the Tm:YbAG AE is given in Fig. 2. The scale of the vertical axis was chosen so that the absorption lines of Tm^{3+} were shown in most detail; in this case, the absorption coefficients of Yb^{3+} lie far above the shown range (0–24 cm^{-1}).

The measurements were performed using a Shimadzu UV-3600 spectrophotometer. About 60% of the pump power was absorbed in the length of the AE. It should be noted that the pump wavelength of 1.678 μm used in our experiments does not match the maximum of the strongest absorption line of Tm^{3+} and, hence, is not optimal for achieving the highest efficiency of the quasi-three-level laser. Thus, the laser efficiency can be increased by choosing a laser pump source compatible with the most intense absorption line of Tm^{3+}.

Yu.D. Zavartsev, A.I. Zagumennyi, Yu.L. Kalachev, S.A. Kutovoi, V.A. Mikhailov, I.A. Shcherbakov A.M. Prokhorov General Physics Institute, Russian Academy of Sciences, ul. Vavilova 38, 119991 Moscow, Russia; e-mail: kalachev@kapella.gpi.ru

Received 28 February 2014
Kvantovaya Elektronika **44** (10) 895–898 (2014)
Translated by M.N. Basieva

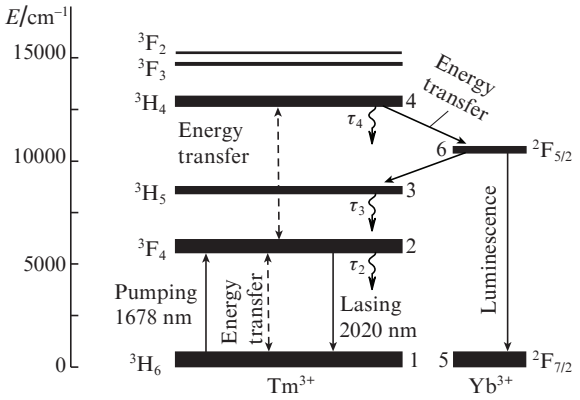

Figure 1. Diagram of low-lying levels of Tm^{3+} and Yb^{3+}.

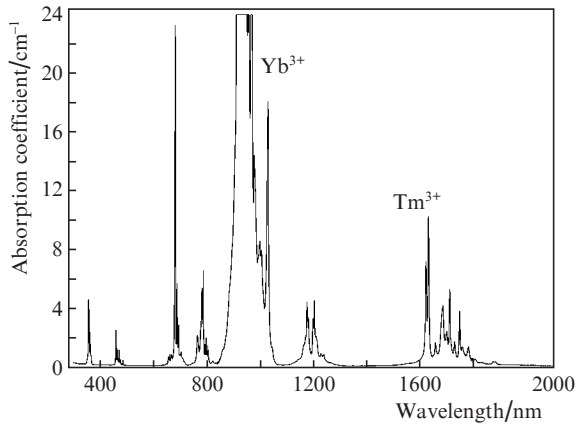

Figure 2. Absorption spectrum of a Tm:YbAG crystal with 5.7 at % of thulium ions. The absorption coefficient of Yb^{3+} in the maximum exceeds 68 cm^{-1}.

The AE luminescence spectra were excited at λ = 1.678 μm. The AE was placed in front of an MDR-204 (LOMO-Fotonika) monochromator. The crystal faces were oriented perpendicular to the optical axis of the monochromator, and the other (frosted) surfaces of the crystal were oriented in the vertical and horizontal planes. The pump laser radiation with a power of 100 mW was focused by a lens with the focal length 80 mm. Thus, we had in the focal region a laser spot 80 μm in diameter with a confocal length of 15 mm. This beam was directed vertically to the upper plane of the crystal so that a luminescence channel was formed in the crystal parallel to its faces at a distance of 15 μm from the face most distant from the monochromator. The luminescence channel image was projected on the monochromator slit by a spherical mirror with a focal length of 20 cm. The crystal axis was lower than the mirror axis to avoid screening of the monochromator slit, and the mirror was inclined at a small angle with respect to the vertical plane. This geometry ensures minimal distortions of luminescence spectra caused by light reabsorption both at the exit from the crystal and due to focusing on the monochromator slit.

The radiation was detected by photodiodes FD-24k at wavelengths shorter than 1 μm and G8373-01 (Hamamatsu) in the wavelength range 1–2.2 μm. The pump radiation was modulated by an MC2000 (Thorlabs) optical chopper within the modulation frequency range 2–1000 Hz. The signal from the photodiodes was amplified by a SR830 (Stanford Research Systems) lock-in amplifier and recorded by a personal computer using the MDR-204 monochromator software. Figure 3 shows the absorption, luminescence, and lasing spectra of the Tm:YbAG crystal. A slight difference in the wavelengths of the absorption and luminescence peaks is caused by the error in the measurement of wavelengths by the monochromator, which was about 1.6 nm.

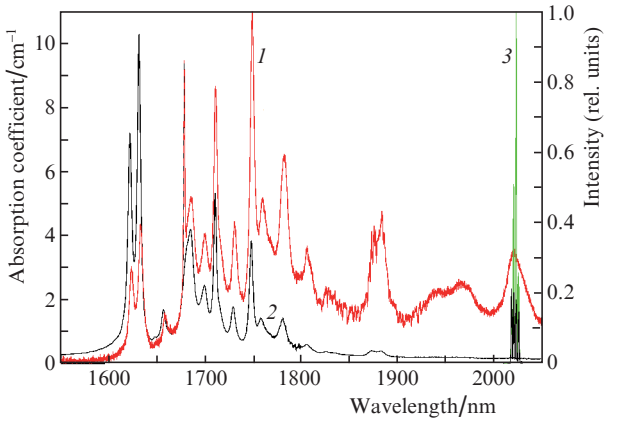

Figure 3. Luminescence (*1*), absorption (*2*), and lasing (*3*) spectra of a Tm:YbAG crystal. The pump wavelength is 1678 nm.

The luminescence spectrum lies in the range 1600–2100 nm, while the lasing spectrum peaked at 2023 nm almost coincides with the long-wavelength luminescence line at $\lambda \sim$ 2020 nm. Taking into account that the absorption of the AE at wavelengths longer than 1800 nm is insignificant, one can expect that the laser wavelength can be tuned in a wide (1800–2100 nm) range when using a spectrally selective cavity. In this case, lasing should be more efficient in the regions of most intense luminescence, at 1880, 1960, and 2020 nm.

4. Luminescence decay time

The two-micron luminescence decay time was calculated by the Bode diagrams – amplitude-frequency (AFCs) and phase-frequency characteristics (PFCs) – measured upon pump beam modulation by a disk chopper in the frequency range 2–1000 Hz (see, for example, [7]). In this frequency range, the main contribution to the Bode diagrams is made by the processes with characteristic times of ~1 ms and larger. For the studied crystal, the longest-lived state is $^3F_4$ with expected lifetime of the order of several milliseconds. The lifetimes of other levels of Tm^{3+} ions are considerably shorter than 1 ms.

The lifetime of the $^3F_{5/2}$ state of Yb^{3+} ions in undoped YbAG crystals was measured in [3] to be 939 μs. In the same work, it was shown that small concentrations of Tm^{3+} or Er^{3+} ions (as unwanted impurities) decrease the lifetime of this level. For example, according to [8], the lifetime of the $^3F_{5/2}$ level is 860 μs.

Thus, we can suggest that the Bode diagrams in the modulation frequency range 2–1000 Hz are determined mainly by the lifetime of the $^3F_4$ level, and the luminescence pulse shape will be described by the expression

$$\frac{U(t)}{U_{\max}} = \begin{cases} 1 - \exp(-t/\tau), & 0 < t < t_p, \\ \exp(t_p - t)/\tau, & t > t_p, \end{cases} \quad (1)$$

where $U(t)$ is the photodetector signal, U_{max} is the steady-stable (maximal) photodetector signal, t_p is the pump pulse duration, and τ is the level lifetime. At a modulation frequency f and an off-duty ratio 2, the pump pulse duration is $t_p = 1/(2f)$. In this case, the Bode diagrams have the form

$$\frac{U(f)}{U_{max}} = \sqrt{\frac{1}{1 + (2\pi f\tau)^2}}, \quad (2)$$

$$\varphi = -\arctan(2\pi f\tau), \quad (3)$$

where φ is the phase shift between the pump pulse and the photodetector signal. From these relations, we can find $\tau = 1/(2\pi F_p)$, where F_p is the frequency at which the phase shift is −45°, and the normalised amplitude is 0.707.

Figure 4 shows the measured and calculated AFCs and PFCs of luminescence at a wavelength of 2020 nm.

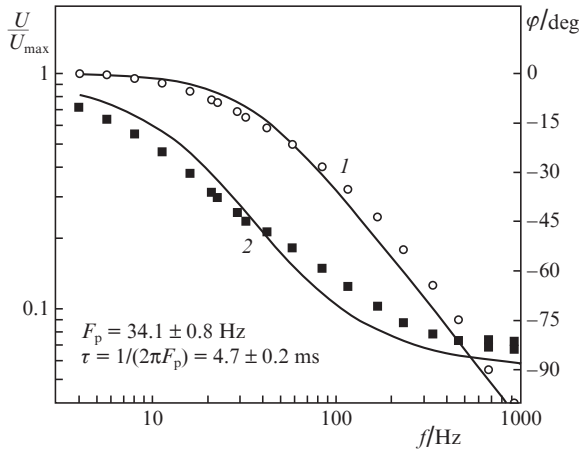

Figure 4. Measured and calculated AFC (*1*) and PFC (*2*) of luminescence at a wavelength of 2020 nm.

Approximation of experimental points by dependences (2) and (3) yields $F_p = 33.7 \pm 1.3$ Hz for AFC and $F_p = 35.9 \pm 2.8$ Hz for PFC. The weight-average frequency is $F_p = 34.1 \pm 0.8$ Hz, which corresponds to the time $\tau = 4.7 \pm 0.2$ ms. Deviations of the AFC and PFC from the theoretical values can be related to the effect of transitions ignored in this model.

5. Laser experiments

Lasing was achieved using a nearly semi-concentric cavity formed by a highly reflecting plane mirror and a spherical output mirror with a curvature radius of 50 mm and a reflection coefficient of 98% at the laser wavelength. The AE was placed near the plane mirror and pumped through the plane dichroic mirror by a single-mode erbium fibre laser with Raman conversion emitting at a wavelength of 1.678 μm.

Figure 5 shows the dependences of the Tm:YbAG laser power on the pump power absorbed in the AE. The measurements were performed in the pulsed and cw regimes. The pulsed regime was achieved by using a disk chopper which was open for 1/20 of the rotation period and rotated with a frequency of 10 Hz.

Laser oscillation occurred at a pump power as low as ~200 mW and was most efficient in the pulsed regime (the slope and total efficiencies were ~41% and 33%, respectively). The output laser power reached 330 mW and was limited only by the maximum possible power of the used pump laser. With increasing pump power, the output laser power monotonically increased without tendency to saturation. It should be noted that the Tm:YbAG crystal demonstrates a high efficiency, which is comparable, under similar conditions, with efficiencies of other well-known highly efficient crystals, for example, Tm:YLF [9]. This points to a promising outlook for the use of Tm:YbAG crystals as laser AEs.

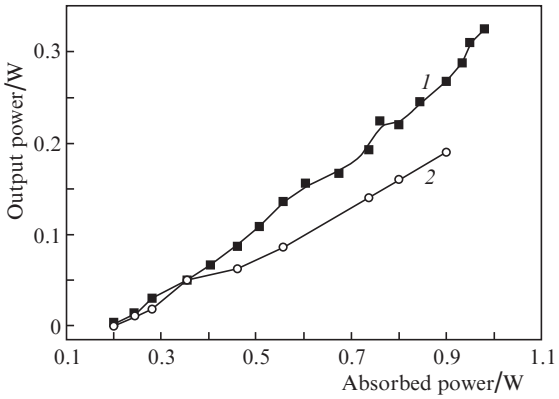

Figure 5. Dependences of the Tm:YbAG laser output power on the pump power absorbed in the AE in the pulsed (*1*) and cw (*2*) regimes.

In the cw pimping regime at a moderate (approximately twofold) excess over the threshold, the laser efficiency is approximately the same as in the pulsed regime. At higher pump powers, the efficiency of cw lasing is by 20%–25% lower than in the pulsed regime. The highest laser power in the cw regime was 180 mW at the slope and total laser efficiencies of 32% and 21%, respectively. The decrease in the laser efficiency observed in the cw regime can be related to heating of a channel in the crystal by the pump radiation. This heating increases the intracavity losses, which is typical for the quasi-three-level laser scheme.

The typical spectra of the Tm:YbAG laser are shown in Fig. 6. They consist of several lines in the range 2017–2027 nm. With increasing pump power, the strongest increase in intensity is observed for the line at 2023 nm, and one more line begins to appear with a centre at $\lambda = 2028$ nm. The presence of equidistant lines in the laser spectrum and the distance between them well agree with the thickness of the intracavity

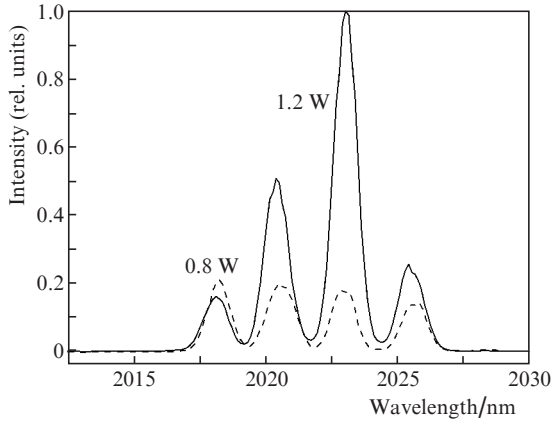

Figure 6. Laser spectra at pump powers of 0.8 and 1.2 W.

Fabry–Perot interferometer formed by the rear cavity mirror ($R \sim 100\%$) and the plane-parallel AE faces without antireflection coating.

Thus, our experiments showed that the new laser crystal Tm:YbAG is rather easy to grow and demonstrates high laser characteristics close to the characteristics of its analogue – Tm:YAG crystal – and well known efficient laser crystals Tm:YLF, Tm:YAP, and others. We obtained efficient lasing in the Tm:YbAG crystal at room temperature within the wavelength range 2017–2027 nm with high total (33%) and slope (41%) efficiencies at the output power of linearly polarised radiation up to ~330 mW, i.e., the energy characteristics of the Tm:YbAG laser are found to be close to the characteristics of the best lasers based on the crystals of this family. The measured 2020-nm luminescence decay time is 4.7 ms. The results of this work testify to a promising outlook for the use of Tm:YbAG AEs in laser engineering.

References

1. Jelinkova H., Koranda P., Sulc J., Nemec M., Cerny P., Pasta J. *Proc. SPIE Int. Soc. Opt. Eng*., **6871**, 68712N (2008).
2. Zavartsev Yu.D., Zagumennyi A.I., Kalachev Yu.L., Kutovoi S.A., Mikhailov V.A., Shcherbakov I.A. *Kvantovaya Elektron*., **43** (11), 989 (2013) [*Quantum Electron*., **43** (11), 989 (2013)].
3. Fagundes-Peters D., Martynyuk N., Lunstedt K., Peters V., Petermann K., Huber G., Basun S., Laguta V., Hofstaetter A. *J. Luminescence*, **125**, 238 (2007).
4. Morris P.J., Luthy W., Weber H.P., Zavartsev Yu.D., Studenikin P.A., Umyskov A.F., Zagumenyi A.I. *Proc. CLEO/EUROPE'94* (Amsterdam, 1994) p. 382
5. Tiseanu C., Lupei A., Lupei V. *J. Phys.: Condens. Matter*, **7**, 8477 (1995).
6. Buchanan R.A., Wickersheim K.A., Pearson J.J., Herrmann G.F. *Phys. Rev*., **159**, 245 (1967).
7. Dorf R., Bishop R. *Modern Control Systems* (New Jersey: Prentice-Hall, 2000).
8. Petermann K., Fagundes-Peters D., Johannsen J., Mond M., Peters V., Romero J.J., Kutovoi S., Speiser J., Giesen A. *J. Cryst. Growth*, **275**, 135 (2005).
9. Kalachev Yu.L., Mihailov V.A., Podreshetnikov V.V., Shcherbakov I.A. *Opt. Commun*., **284**, 3357 (2011).